

Hydrogen Atom Abstraction and Hydride Transfer Reactions by Iron(IV)–Oxo Porphyrins**

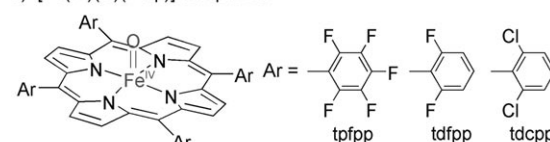
Yu Jin Jeong, Yaeun Kang, Ah-Rim Han, Yong-Min Lee, Hiroaki Kotani, Shunichi Fukuzumi,* and Wonwoo Nam*

High-valent iron(IV)–oxo species are frequently invoked as the key oxidizing intermediates in the catalytic cycles of heme and nonheme iron enzymes.^[1–3] In heme iron enzymes, high-valent iron(IV)–oxo species are proposed as reactive intermediates in dioxygen activation and oxygen-atom transfer reactions, such as iron(IV)–oxo porphyrin π -radical cations, referred to as compound I, and iron(IV)–oxo porphyrins, referred to as compound II.^[1] Whereas the reactivity of compound I has been well investigated with synthetic iron porphyrins in various oxidation reactions,^[1,2c,4] compound II has been rarely used as an oxidant because of its low oxidizing power in nature.^[5]

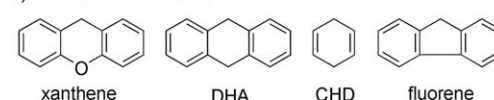
Very recently, we have observed significant progress in understanding the reactivities of mononuclear nonheme iron(IV)–oxo complexes, which are analogues to compound II in heme enzymes, in a variety of oxidation reactions,^[2,6–8] including the activation of C–H bonds of alkanes and alkyl aromatics.^[7] As part of our efforts to elucidate the reactivities and mechanisms of iron(IV)–oxo complexes of heme and nonheme ligands in oxidation reactions, we performed hydrogen-atom abstraction (H-atom abstraction) and hydride-transfer reactions with iron(IV)–oxo porphyrins generated in situ (Scheme 1). Herein, we report the first examples of C–H bond activation of alkyl aromatics and hydride transfer of dihydronicotinamide adenine dinucleotide (NADH) analogues by iron(IV)–oxo porphyrin complexes. The nature of the active oxidant(s), such as an iron(IV)–oxo porphyrin versus an iron(IV)–oxo porphyrin π -radical cation, in the C–H bond activation and hydride-transfer reactions is also discussed.

Iron(IV)–oxo porphyrin complexes [Fe^{IV}(O)(tpfpp)] (**1**; tpfpp = *meso*-tetrakis(pentafluorophenyl)porphinato di-

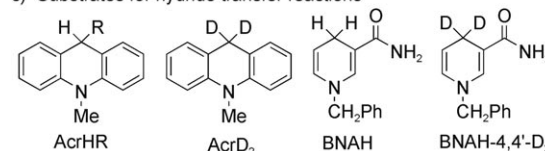
a) [Fe(IV)(O)(Porp)] complexes



b) Substrates for H-abstraction reactions

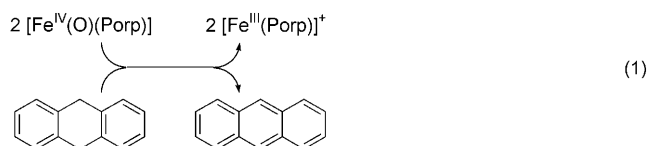


c) Substrates for hydride transfer reactions



Scheme 1. Iron(IV)–oxo porphyrins and substrates used in this study.

anion), [Fe^{IV}(O)(tdfpp)] (**2**; tdfpp = *meso*-tetrakis(2,6-difluorophenyl)porphinato dianion), and [Fe^{IV}(O)(tdcpp)] (**3**; tdcpp = *meso*-tetrakis(2,6-dichlorophenyl)porphinato dianion) (Scheme 1a) were prepared by treating the iron(III) porphyrin chlorides with *meta*-chloroperbenzoic acid (*m*-CPBA) in the presence of a small amount of H₂O in a solvent mixture of CH₃CN and CH₂Cl₂ (9:1) at 15 °C.^[5] Subsequently, the iron(IV)–oxo complexes were used in the oxidation of alkyl aromatics with weak C–H bonds, such as xanthene (75.5 kcal mol^{−1}), 9,10-dihydroanthracene (DHA) (77 kcal mol^{−1}), 1,4-cyclohexadiene (CHD) (78 kcal mol^{−1}), and fluorene (80 kcal mol^{−1}) (Scheme 1b).^[9] Upon addition of substrates to a reaction solution of **1**, the iron(IV)–oxo porphyrin complex reverted back to the starting iron(III) porphyrin complex, showing isosbestic points at 472, 526, and 566 nm in the UV/Vis spectrum (Figure 1a). Product analysis of the reaction solutions revealed that xanthene (40 ± 8% based on the amount of **1** formed), anthracene (42 ± 7%), benzene (41 ± 7%), and 9-fluorenone (26 ± 5%) were yielded as major products in the reactions of xanthene, DHA, CHD, and fluorene, respectively [see Eq. (1) for the oxidation of DHA by **1**]. Fitting the kinetic data for the pseudo-first-order decay of **1** allowed us to determine *k*_{obs} values, and plotting



[*] Dr. H. Kotani, Prof. Dr. S. Fukuzumi
Department of Material and Life Science
Graduate School of Engineering, Osaka University
SORST (Japan) Science and Technology Agency (JST)
Suita, Osaka 565-0871 (Japan)
Fax: (+81) 6-6879-7370
E-mail: fukuzumi@chem.eng.osaka-u.ac.jp

Y. J. Jeong,^[+] Y. Kang,^[+] A.-R. Han, Dr. Y.-M. Lee, Prof. Dr. W. Nam
Department of Chemistry and Nano Science
Ewha Womans University, Seoul 120-750 (Korea)
Fax: (+82) 2-3277-4441
E-mail: wwnam@ewha.ac.kr

[+] These authors contributed equally to this work.

[**] The research at EWU was supported by KOSEF/MOST through the CRI Program, Korea, and the research at OU was supported by a Grant-in-Aid (No. 19205019) from the Ministry of Education, Culture, Sports, Science and Technology (Japan).

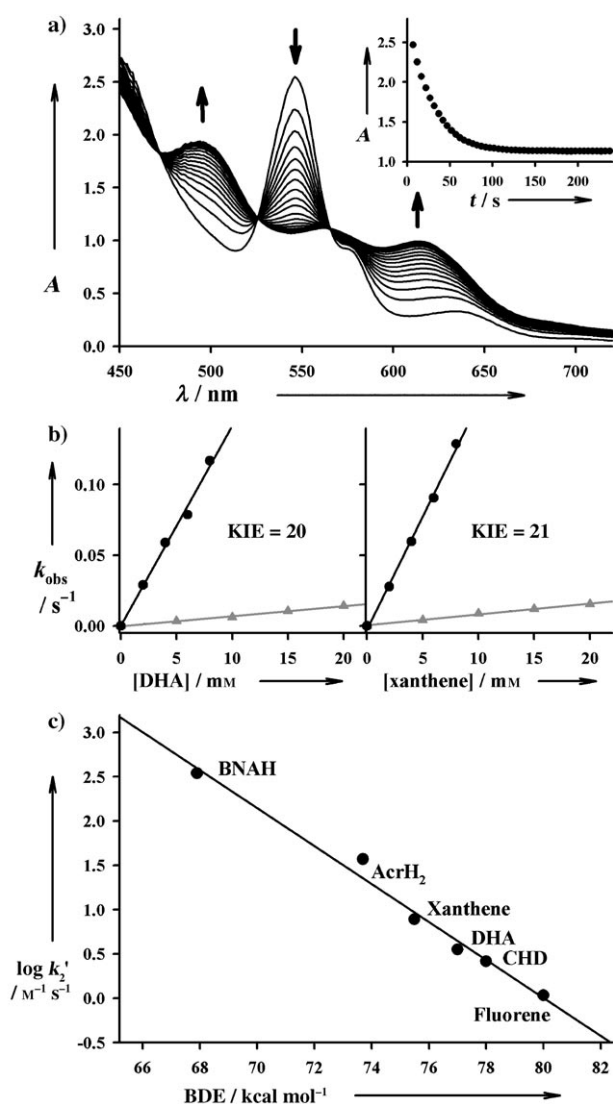


Figure 1. Reactions of **1** with substrates at 15 °C. a) UV/Vis spectral changes of **1** (0.2 mM) upon addition of [D₂]xanthene (20 mM). Inset shows time course of the decay of **1** monitored at $\lambda = 547$ nm. b) Plot of k_{obs} against the concentration of DHA and [D₄]DHA (left panel) and xanthene and [D₂]xanthene (right panel) to determine second-order rate constants. Circles indicate the oxidation of xanthene and DHA; triangles indicate the oxidation of [D₂]xanthene and [D₄]DHA. c) Plot of $\log k_2'$ of **1** against C–H BDE of substrates. Second-order rate constants k_2 were determined at 15 °C and then adjusted for reaction stoichiometry to yield k_2' based on the number of equivalent target C–H bonds of substrates (e.g., 4 for DHA and CHD and 2 for BNAH, AcrH₂, xanthene, and fluorene).

the pseudo-first-order rate constants against the concentration of substrates led us to determine second-order rate constants for the reactions of xanthene ($k_2 = 14 \pm 2 \text{ M}^{-1} \text{ s}^{-1}$), DHA ($k_2 = 13 \pm 2 \text{ M}^{-1} \text{ s}^{-1}$), CHD ($k_2 = 9.0 \pm 0.8 \text{ M}^{-1} \text{ s}^{-1}$), and fluorene ($k_2 = 2.3 \pm 0.2 \text{ M}^{-1} \text{ s}^{-1}$) (Figure 1b for the reactions of DHA and xanthene). As expected, the rate constants decrease with an increase in the C–H bond dissociation energy (BDE) of the substrates, and Figure 1c shows a linear correlation between the $\log k_2'$ values and the C–H BDE values of the substrates (the k_2 values are divided by the number of equivalent target C–H bonds of substrates to

obtain the k_2' values).^[10] These results indicate that an H-atom abstraction is the rate-determining step for the C–H bond activation of alkyl aromatics. Further evidence supporting the H-atom abstraction mechanism was obtained from measurements of the kinetic isotope effect (KIE) of the oxidation of DHA and xanthene, in which KIE values of approximately 20 were obtained in those reactions (Figure 1b). Large KIE values (e.g., 10–20) were observed also in the oxidation of DHA and xanthene by nonheme iron(IV)–oxo complexes, $[\text{Fe}^{\text{IV}}(\text{O})(\text{tmc})(\text{X})]^{n+}$ (tmc = 1,4,8,11-tetramethyl-1,4,8,11-tetraazacyclotetradecane; X = NCCH₃ or anion), for which an H-atom abstraction mechanism was proposed for the C–H bond activation reactions.^[7b] With the results of the good correlation between reaction rates and BDE of substrates and the large KIE values, we propose that the C–H bond oxidation of alkyl aromatics by iron(IV)–oxo porphyrins occurs through an H-atom abstraction mechanism.

The hydride transfer from NADH analogues 10-methyl-9,10-dihydroacridine (AcrH₂), 1-benzyl-1,4-dihydronicotinamide (BNAH), and their derivatives (Scheme 1c),^[11–13] to iron(IV)–oxo porphyrins was also investigated under the conditions of H-atom abstraction reactions. Addition of substrates to a solution of **1** converted the intermediate into the starting iron(III) porphyrin complex (see Figure S1a in the Supporting Information). Pseudo-first-order rate constants, determined by the fitting the kinetic data for the decay of **1**, increased linearly with the increase of the substrate concentration, leading us to determine second-order rate constants of $75 \pm 3 \text{ M}^{-1} \text{ s}^{-1}$ for AcrH₂ and $7.0 \times 10^2 \pm 30 \text{ M}^{-1} \text{ s}^{-1}$ for BNAH (see Figure S1b in the Supporting Information). Interestingly, the reaction rates of AcrH₂ and BNAH were well-fitted into the plot of $\log k_2$ and BDE of AcrH₂ (73.7 kcal mol^{−1}) and BNAH (67.9 kcal mol^{−1}) (see Figure 1c).^[12,14] Further, we have obtained large KIE values of 17 and 8.6 for the reactions of AcrH₂ and BNAH, respectively (see Figure S1b in the Supporting Information). These results demonstrate that the C–H bond activation of NADH analogues is involved as a rate-determining step in the hydride transfer reactions by iron(IV)–oxo porphyrins. Furthermore, when we compared the reactivities of **1** and *p*-chloranil (Cl₄Q) in hydride-transfer reactions of NADH analogues (see Table S1 in the Supporting Information), we observed a good linear correlation between the k_2 values of **1** and the corresponding values of Cl₄Q (Figure 2).^[15] Such a linear correlation between the $\log k_2$ values of $[\text{Fe}^{\text{IV}}(\text{O})(\text{Porp})]$ and the corresponding values of Cl₄Q suggests that hydride transfer from NADH analogues to $[\text{Fe}^{\text{IV}}(\text{O})(\text{Porp})]$ proceeds through hydrogen-atom transfer, which is regarded as proton-coupled electron transfer (PCET) from AcrH₂ to $[\text{Fe}^{\text{IV}}(\text{O})(\text{Porp})]$,^[11a,12,16] followed by rapid electron transfer from the resulting AcrH[•] to an $[\text{Fe}^{\text{IV}}(\text{O})(\text{Porp})]$ molecule to afford the AcrH⁺ product, as in the proposed mechanism depicted in Scheme 2.

We then investigated the porphyrin ligand effect on the reactivities of $[\text{Fe}^{\text{IV}}(\text{O})(\text{Porp})]$ in the H-atom abstraction and hydride-transfer reactions (see Scheme 1a for porphyrin ligands). In the oxidation of xanthene, second-order rate constants of 14 ± 2 , 11 ± 2 , and $1.6 \pm 0.2 \text{ M}^{-1} \text{ s}^{-1}$ were determined in the reactions of **1**, **2**, and **3**, respectively, indicating

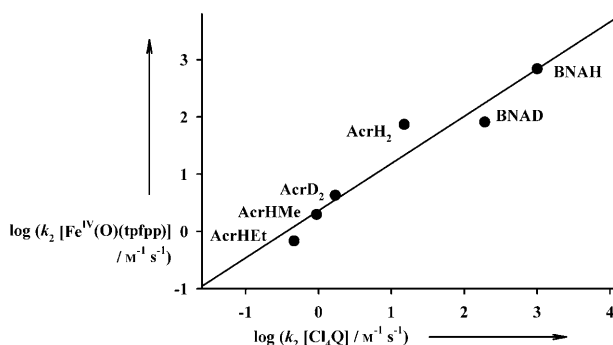
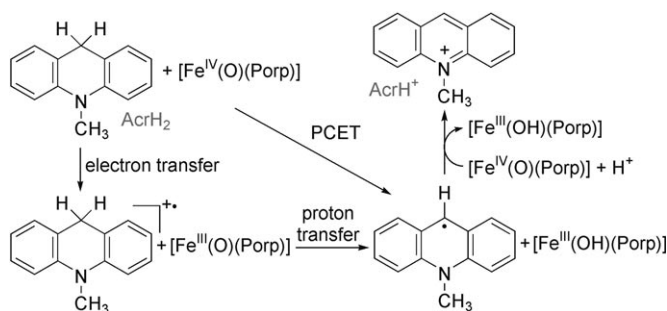


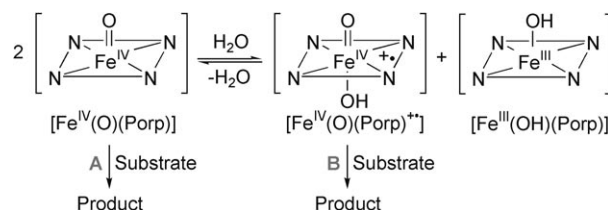
Figure 2. Plots of $\log k_2$ for hydride transfer from NADH analogues to **1** at 15°C vs. $\log k_2$ for hydride transfer from the same series of NADH analogues to Cl_4Q at 25°C.



Scheme 2. Proposed mechanism of hydride transfer reaction.

that an iron(IV)–oxo complex bearing a more electron-deficient porphyrin ligand is a more powerful oxidant in the activation of C–H bonds.^[17] Similarly, an iron(IV)–oxo species bearing a more electron-deficient porphyrin ligand showed a slightly greater reactivity in the hydride-transfer reaction (i.e., $k_2 = 75 \pm 5$, 43 ± 3 , and $25 \pm 3 \text{ M}^{-1} \text{ s}^{-1}$ for the reactions of **1**, **2**, and **3**, respectively, with AcrH_2). Interestingly, the reactivity order **1** > **2** > **3** in the H-atom abstraction and hydride-transfer reactions is different from that reported in the oxidation of olefins and benzylic alcohols by the iron(IV)–oxo porphyrins; in the latter reactions, an inverted reactivity order **3** > **2** > **1** was reported.^[18a] On the basis of the inverted reactivity of iron(IV)–oxo porphyrins, Pan and Newcomb proposed that the true active oxidant in the oxidation of olefins and benzylic alcohols by iron(IV)–oxo porphyrins is iron(IV)–oxo porphyrin π -radical cations ($[\text{Fe}^{\text{IV}}(\text{O})(\text{Porp})^{\bullet+}]$), which were generated by the disproportionation of the iron(IV)–oxo species (Scheme 3).^[18] Thus, we carried out mechanistic studies to understand the nature of active oxidant(s) in the C–H bond oxidation and hydride-transfer reactions by iron(IV)–oxo porphyrins (e.g., Scheme 3, pathway A vs. pathway B).

First, the reactivity orders in the oxidation of alkyl aromatics and NADH analogues follow the typical electrophilic reaction; an electron-deficient iron(IV)–oxo species shows a greater reactivity, although the reactivity difference depending on the porphyrin ligands is not significant.^[19] Second, whereas $[\text{Fe}^{\text{IV}}(\text{O})(\text{tpfpp})^{\bullet+}]$ hydroxylates cyclooctane ($95.7 \text{ kcal mol}^{-1}$) at -30°C ,^[17] **1** does not react with



Scheme 3. Proposed mechanism for the oxidation of organic substrates by iron(IV)–oxo porphyrins.

the substrate even at 25°C (data not shown). If **1** is disproportionated to $[\text{Fe}^{\text{IV}}(\text{O})(\text{tpfpp})^{\bullet+}]$ and $[\text{Fe}^{\text{III}}(\text{tpfpp})^+]$ through an equilibrium^[18,20] and $[\text{Fe}^{\text{IV}}(\text{O})(\text{tpfpp})^{\bullet+}]$ is the true oxidant, then we should observe the decay of **1** because $[\text{Fe}^{\text{IV}}(\text{O})(\text{tpfpp})^{\bullet+}]$ reacts very rapidly with cyclooctane at 25°C and **1** is used in generating the $[\text{Fe}^{\text{IV}}(\text{O})(\text{tpfpp})^{\bullet+}]$ intermediate by the disproportionation process (Scheme 3). Similarly, whereas **1** disappears in the reaction of CHD at -20°C , it remains intact upon the addition of ethylbenzene (86 kcal mol^{-1}) (see Figure S2 in the Supporting Information). As we have discussed above, if the oxidation of CHD by **1** occurs by $[\text{Fe}^{\text{IV}}(\text{O})(\text{tpfpp})^{\bullet+}]$ generated by the disproportionation process (Scheme 3, pathway B), the disappearance of **1** should be observed in the ethylbenzene hydroxylation as well. Thus, the results that **1** reacts with CHD but not with ethylbenzene indicate that **1** is not a strong oxidant but is capable of oxidizing CHD under the present reaction conditions. Finally, since it has been shown that the oxidation of substrates by iron(IV)–oxo species was suppressed by the presence of iron(III) porphyrins because of the equilibrium shift towards the inhibition of the generation of the true oxidant (i.e., $[(\text{Porp})^{\bullet+}\text{Fe}^{\text{IV}}=\text{O}]^+$),^[18] we carried out the oxidation of xanthene and the hydride transfer of AcrH_2 by adding two equivalents of $[\text{Fe}^{\text{III}}(\text{tpfpp})^+]$ to the reaction solution of **1** and found that reaction rates were not affected by the presence of $[\text{Fe}^{\text{III}}(\text{tpfpp})^+]$. These results indicate that there is no disproportionation of **1** to $[(\text{Porp})^{\bullet+}\text{Fe}^{\text{IV}}=\text{O}]^+$ and $[\text{Fe}^{\text{III}}(\text{tpfpp})^+]$ and that **1**, not $[(\text{Porp})^{\bullet+}\text{Fe}^{\text{IV}}=\text{O}]^+$, is the true active oxidant responsible for the weak C–H bond activation of alkyl aromatics and the hydride transfer of NADH analogues under our reaction conditions.

In conclusion, we have reported two important findings in the reactivity studies of iron(IV)–oxo porphyrin complexes. First, we have shown that iron(IV)–oxo porphyrins are competent oxidants in the oxidations of alkyl aromatics and NADH analogues and that the oxidation reactions occur through H-atom abstraction and PCET mechanisms, respectively. Second, we have demonstrated that the active oxidant responsible for the activation of weak C–H bonds and the hydride transfer of NADH analogues is iron(IV)–oxo porphyrins, but not iron(IV)–oxo porphyrin π -radical cations.

Received: May 20, 2008

Published online: August 7, 2008

Keywords: C–H activation · enzyme models · hydride transfer · iron · oxo ligands

- [1] a) R. van Eldik, *Coord. Chem. Rev.* **2007**, *251*, 1649–1662; b) P. R. Ortiz de Montellano, *Cytochrome P450: Structure, Mechanism, and Biochemistry*, 3rd ed., Kluwer Academic/Plenum Publishers, New York, **2005**; c) I. G. Denisov, T. M. Makris, S. G. Sligar, I. Schlichting, *Chem. Rev.* **2005**, *105*, 2253–2277; d) B. Meunier, S. P. de Visser, S. Shaik, *Chem. Rev.* **2004**, *104*, 3947–3980.
- [2] a) C. Krebs, D. G. Fujimori, C. T. Walsh, J. M. Bollinger, Jr., *Acc. Chem. Res.* **2007**, *40*, 484–492; b) W. Nam, *Acc. Chem. Res.* **2007**, *40*, 522–531.
- [3] a) M. M. Abu-Omar, A. Loaiza, N. Hontzas, *Chem. Rev.* **2005**, *105*, 2227–2252; b) S. V. Kryatov, E. V. Rybak-Akimova, S. Schindler, *Chem. Rev.* **2005**, *105*, 2175–2226.
- [4] a) Z. Gross, S. Nimri, *Inorg. Chem.* **1994**, *33*, 1731–1732; b) W. J. Song, Y. O. Ryu, R. Song, W. Nam, *J. Biol. Inorg. Chem.* **2005**, *10*, 294–304.
- [5] a) W. Nam, S.-E. Park, I. K. Lim, M. H. Lim, J. Hong, J. Kim, *J. Am. Chem. Soc.* **2003**, *125*, 14674–14675; b) K. Nehru, M. S. Seo, J. Kim, W. Nam, *Inorg. Chem.* **2007**, *46*, 293–298.
- [6] a) J.-U. Rohde, J.-H. In, M. H. Lim, W. W. Brennessel, M. R. Bukowski, A. Stubna, E. Münck, W. Nam, L. Que, Jr., *Science* **2003**, *299*, 1037–1039; b) M. R. Bukowski, K. D. Koehntop, A. Stubna, E. L. Bominaar, J. A. Halfen, E. Münck, W. Nam, L. Que, Jr., *Science* **2005**, *310*, 1000–1002; c) C. V. Sastri, K. Oh, Y. J. Lee, M. S. Seo, W. Shin, W. Nam, *Angew. Chem.* **2006**, *118*, 4096–4099; *Angew. Chem. Int. Ed.* **2006**, *45*, 3992–3995.
- [7] a) J. Kaizer, E. J. Klinker, N. Y. Oh, J.-U. Rohde, W. J. Song, A. Stubna, J. Kim, E. Münck, W. Nam, L. Que, Jr., *J. Am. Chem. Soc.* **2004**, *126*, 472–473; b) C. V. Sastri, J. Lee, K. Oh, Y. J. Lee, J. Lee, T. A. Jackson, K. Ray, H. Hirao, W. Shin, J. A. Halfen, J. Kim, L. Que, Jr., S. Shaik, W. Nam, *Proc. Natl. Acad. Sci. USA* **2007**, *104*, 19181–19186.
- [8] a) V. Bolland, M.-F. Charlot, F. Banse, J.-J. Girerd, T. A. Mattioli, E. Bill, J.-F. Bartoli, P. Battioni, D. Mansuy, *Eur. J. Inorg. Chem.* **2004**, 301–308; b) J. Bautz, P. Comba, C. L. de Laorden, M. Menzel, G. Rajaraman, *Angew. Chem.* **2007**, *119*, 8213–8216; *Angew. Chem. Int. Ed.* **2007**, *46*, 8067–8070.
- [9] a) J. M. Mayer, *Biomimetic Oxidations Catalyzed by Transition Metal Complexes* (Ed.: B. Meunier), Imperial College Press, London, **2000**, pp. 1–43; b) J. P. Roth, J. M. Mayer, *Inorg. Chem.* **1999**, *38*, 2760–2761.
- [10] a) J. M. Mayer, *Acc. Chem. Res.* **1998**, *31*, 441–450; b) A. S. Borovik, *Acc. Chem. Res.* **2005**, *38*, 54–61; c) W. W. Y. Lam, S.-M. Yiu, D. T. Y. Yiu, T.-C. Lau, W.-P. Yip, C.-M. Che, *Inorg. Chem.* **2003**, *42*, 8011–8018; d) C. R. Goldsmith, A. P. Cole, T. D. P. Stack, *J. Am. Chem. Soc.* **2005**, *127*, 9904–9912.
- [11] a) S. Fukuzumi, K. Ohkubo, Y. Tokuda, T. Suenobu, *J. Am. Chem. Soc.* **2000**, *122*, 4286–4294; b) S. Fukuzumi, K. Ohkubo, T. Okamoto, *J. Am. Chem. Soc.* **2002**, *124*, 14147–14155; c) J. Yuasa, S. Yamada, S. Fukuzumi, *J. Am. Chem. Soc.* **2006**, *128*, 14938–14948.
- [12] a) T. Matsuo, J. M. Mayer, *Inorg. Chem.* **2005**, *44*, 2150–2158; b) S. Fukuzumi, Y. Tokuda, T. Kitano, T. Okamoto, J. Otera, *J. Am. Chem. Soc.* **1993**, *115*, 8960–8968.
- [13] a) X.-Q. Zhu, Y. Yang, M. Zhang, J.-P. Cheng, *J. Am. Chem. Soc.* **2003**, *125*, 15298–15299; b) X.-Q. Zhu, L. Cao, Y. Liu, Y. Yang, J.-Y. Lu, J.-S. Wang, J.-P. Cheng, *Chem. Eur. J.* **2003**, *9*, 3937–3945; c) O. Pestovsky, A. Bakac, J. H. Espenson, *J. Am. Chem. Soc.* **1998**, *120*, 13422–13428.
- [14] X.-Q. Zhu, H.-R. Li, Q. Li, T. Ai, J.-Y. Lu, Y. Yang, J.-P. Cheng, *Chem. Eur. J.* **2003**, *9*, 871–880.
- [15] Detailed discussion of the linear correlation observed in hydride-transfer reactions by high-valent metal-oxo species and Cl₄Q will be presented in elsewhere: S. Fukuzumi, H. Kotani, Y.-M. Lee, W. Nam, unpublished results.
- [16] The proton source for the proton-transfer step in Scheme 2 is H₂O added into the reaction solution to generate [Fe^{IV}(O)-(Porp)].
- [17] Y. M. Goh, W. Nam, *Inorg. Chem.* **1999**, *38*, 914–920.
- [18] a) Z. Pan, M. Newcomb, *Inorg. Chem.* **2007**, *46*, 6767–6774; b) R. Zhang, M. Newcomb, *Acc. Chem. Res.* **2008**, *41*, 468–477.
- [19] a) N. A. Stephenson, A. T. Bell, *J. Mol. Catal. A* **2007**, *275*, 54–62, and references therein; b) H. Fujii, *Coord. Chem. Rev.* **2002**, *226*, 51–60; c) D. Dolphin, T. G. Traylor, L. Y. Xie, *Acc. Chem. Res.* **1997**, *30*, 251–259.
- [20] M. Wolak, R. van Eldik, *Chem. Eur. J.* **2007**, *13*, 4873–4883.